Iranian Journal of Basic Medical Sciences
ijbms.mums.ac.ir

Down-regulation of AGXT2L1 promotes the development of nonalcoholic fatty liver disease

Yue Yu [1], Lu Wu [1]*

[1] Department of Radiation Oncology, Guangdong Provincial People's Hospital (Guangdong Academy of Medical Sciences), Southern Medical University, Guangzhou, China

ARTICLE INFO

Article type:
Original

Article history:
Received: Aug 23, 2025
Accepted: Jun 7, 2026

Keywords:
Alanine-glyoxylate-aminotransferase 2-like1-(AGXT2L1)
Apoptosis
ER stress
Inflammation
Nonalcoholic fatty - liver disease (NAFLD)
Phospholipid metabolism

ABSTRACT

Objective(s): To investigate the role of alanine-glyoxylate aminotransferase 2-like1 (AGXT2L1) in Nonalcoholic fatty liver disease (NAFLD) and its underlying mechanisms.

Materials and Methods: Changes in AGXT2L1 expression during NASH progression were analyzed using tissue samples, cell experiments, and animal models. RNA sequencing was performed on experimental mice to explore potential mechanisms by assessing inflammatory factors, cell apoptosis, and endoplasmic reticulum stress.

Results: Compared with normal tissues, AGXT2L1 expression was reduced in multiple liver diseases. Both *in vitro* and *in vivo* experiments confirmed that down-regulation of AGXT2L1 exacerbated NASH severity. RNA sequencing initially indicated that abnormal AGXT2L1 expression primarily affects phospholipid metabolism. Additionally, animal experiments showed that AGXT2L1 deficiency increased the number of apoptotic hepatocytes and elevated the expression of endoplasmic reticulum stress markers.

Conclusion: Decreased AGXT2L1 expression is an evident alteration in liver injury. It has been indicated that down-regulation of AGXT2L1 promotes NAFLD development, possibly through three pathways: activation of inflammatory responses, promotion of hepatocyte apoptosis, and enhancement of endoplasmic reticulum stress.

▶ Please cite this article as:
Yu Y, Wu L. Down-regulation of AGXT2L1 promotes the development of nonalcoholic fatty liver disease. Iran J Basic Med Sci 2026; 29: 1390-1397. doi: https://dx.doi.org/10.22038/ijbms.2026.89567.19546

Introduction

The global prevalence of chronic liver disease has increased annually. With poor long-term clinical efficacy, it has become a major cause of morbidity and mortality, posing a severe threat to human health (1, 2). Nonalcoholic fatty liver disease (NAFLD) is a metabolic stress-induced liver injury disorder that encompasses a spectrum of conditions, from simple steatosis to nonalcoholic steatohepatitis (NASH)(3, 4). If NAFLD progresses to steatohepatitis, it may lead to cirrhosis, end-stage liver disease, or even hepatocellular carcinoma (5). NASH is associated with poor prognosis and limited treatment options, with most therapies yielding suboptimal clinical outcomes and survival rates (6). Therefore, exploring the key genes and molecular mechanisms underlying NASH progression is essential to provide new insights for the development of targeted drugs and therapeutic strategies.

In recent years, novel mechanisms of NAFLD pathogenesis have been continuously elucidated and refined, positing that genetic factors, gut microbiota dysbiosis, lipid metabolic disorders, and oxidative stress contribute to different stages of NAFLD development (7, 8). Researchers have identified a critical role of the synthesis and metabolism of phosphatidylethanolamine (PE) and phosphatidylcholine (PC)(both present in hepatocyte membranes) in NAFLD pathogenesis (9). In some mouse models, increased PE synthesis or impaired conversion of PE to PC has been shown to promote the progression of NAFLD (10, 11). On one hand, a relative increase in membrane PE disrupts membrane homeostasis (12), alters hepatocellular lipid droplet formation, impairs mitochondrial respiratory chain function, and induces endoplasmic reticulum stress (13, 14). On the other hand, a reduced PC/PE ratio increases membrane permeability, leading to leakage of intracellular contents, activation of inflammatory responses, and production of reactive oxygen species (ROS)—all of which drive NAFLD pathogenesis (15, 16). Despite extensive research on genes associated with the development of NAFLD, the mechanisms underlying its pathological changes and progression remain poorly understood.

The alanine-glyoxylate aminotransferase 2-like 1 (AGXT2L1) gene is located on human chromosome 4q25 and is named for its 36% sequence identity to AGXT2 (alanine-glyoxylate aminotransferase 2) (17). AGXT2L1 exhibits phosphohydrolytic activity toward phosphoethanolamine (P-Etn), irreversibly degrading P-Etn into acetaldehyde, phosphate, and ammonia; thus, it is also referred to as ethanolamine-phosphate phospho-lyase (ETNPPL)(18). Studies have shown that PE metabolism is closely associated

***Corresponding author:** Lu Wu. Department of Radiation Oncology, Guangdong Provincial People's Hospital (Guangdong Academy of Medical Sciences), Southern Medical University, Guangzhou, China. Tel/ Fax: +20-8382781251221, Email: melody80017@163.com

with NASH occurrence and severity. Given that AGXT2L1 is a key degrading enzyme for P-Etn (the direct substrate for PE synthesis), we hypothesized that reduced AGXT2L1 expression would cause liver cell damage, potentially inducing or exacerbating hepatic steatosis in the context of diet-induced NAFLD.

Previous studies have linked abnormal AGXT2L1 expression to prognosis in hepatocellular carcinoma patients (19) and suggested its involvement in lipid metabolism; however, no research has explored its role in NASH. Based on the functional characteristics of AGXT2L1 and the critical role of PE metabolism in NASH progression (e.g., reduced hepatic PE synthesis alters the PC/PE ratio and triggers adverse effects, while increased hepatocellular PE levels alleviate hepatic steatosis)(20), we propose that decreased AGXT2L1 expression may slow P-Etn hydrolysis, leading to increased PE synthesis. Alterations in PE levels may disrupt hepatocyte membrane stability and permeability, thereby inducing or accelerating the development of NAFLD. We hypothesize that AGXT2L1 may participate in NAFLD progression. Thus, this study aimed to investigate the role and potential mechanisms of abnormal AGXT2L1 expression in NASH, providing new insights for the precision treatment of this disease.

Materials and Methods

Download of GEO datasets

GEO datasets were retrieved and downloaded from the following website: http://www.ncbi.nlm.nih.gov/gds. Relevant data within the datasets were then organized and analyzed.

Immunohistochemical staining and scoring

Tissue microarrays containing hepatocellular carcinoma and cirrhosis samples were purchased from Xi'an Elina Biotechnology Co., Ltd. for immunohistochemical experiments. After procedures including baking, dewaxing, hydration, antigen retrieval, and blocking, diluted AGXT2L1 primary antibody (1:150 dilution) was added to the sections. Subsequent steps included incubation with a secondary antibody, color development, counterstaining, dehydration, and mounting to complete immunohistochemical staining.

AGXT2L1 expression levels were evaluated using the following formula: Immunohistochemical staining score = (+) % × 1 + (++) % × 2 + (+++) % × 3. Staining intensity was graded as follows: negative (-), 0 points; weak positive (+), 1 point; moderate positive (++), 2 points; strong positive (+++), 3 points. The "%" represents the percentage of positive cells relative to the total number of cells. AGXT2L1 expression was classified based on the score: low expression if the immunohistochemical staining score (ISS) ≤ 1.5, and high expression if ISS > 1.5.

Transient siRNA transfection of cells

Sequences for AGXT2L1 small interfering RNA (AGXT2L1-siRNA) and negative control siRNA (NC-siRNA) were synthesized by GenePharma Co., Ltd. The sequences are listed below: Sequence (5'-3'): AGXT2L1-siRNA-sense: GGAGGAUAUCCAGUAUCUUTT; AGXT2L1-siRNA-antisense: AAGAUAUGGAUUUCCUCCTT; NC-siRNA-sense: UUCUCCGAACGUGUCACGUTT; NC-siRNA -antisense: ACGUGACACGUUCGGAGAATT (21).

Cells were seeded in 6-well plates 1 day before transfection to achieve 30-50% confluency on the day of transfection. Culture medium containing siRNA was added to the 6-well plates for transfection. RNA was extracted after 24-48 hr of culture, and protein was extracted after 48-72 hr.

Oil Red O staining for intracellular lipid droplets

Cells were uniformly seeded in 6-well plates. A 0.6 mg/mL oleic acid solution (1 µl per well) was added, and cells were cultured for an additional 24 hr. Cells were fixed with 4% paraformaldehyde, stained with prepared Oil Red O solution for 1 hr, and excess dye was washed away. Subsequently, 1 mL of hematoxylin dye was added to each well, excess dye was removed, and sections were mounted and observed (19).

Western blot analysis

Prepared protein samples (40 µg total protein per sample) and protein markers were loaded into wells using a micropipette. SDS-PAGE gel electrophoresis was performed for 1.5 hr, and target bands were excised based on the marker for transfer to a membrane (200 mA, 90 min). The membrane was blocked on a shaker at room temperature for 2 hr, then developed. Images were captured using a BIO-RAD gel imaging system.

Grouping and treatment of mice

C57BL/6 mice were used as experimental animals. AGXT2L1 knockout (KO) C57BL/6 mice were purchased from Cyagen Biosciences Inc. (Guangzhou), while wild-type (WT) C57BL/6 mice were obtained from Beijing Vital River Laboratory Animal Technology Co., Ltd.

Sixteen WT mice and 16 KO mice (6-8 weeks old, housed under specific pathogen-free (SPF) conditions) were used. The experiment was divided into four groups (n=8 per group): WT control group (WT-Control, fed a normal diet), WT model group (WT-MCD, fed a methionine-choline-deficient (MCD) diet), KO control group (KO-Control, fed a normal diet), and KO model group (KO-MCD, fed an MCD diet). All other conditions were standardized. Mice were monitored daily for food/water intake, behavior, mental status, and excrement (22).

After 4 weeks of modeling, mice were fasted for 12 hr before sample collection. Instruments (scissors, forceps, gauze, syringes, blood collection tubes, centrifuge tubes) and reagents (PBS, 4% paraformaldehyde) were prepared. Mouse body weight was measured and recorded, followed by blood collection via enucleation of the eyeball. Mice were then dissected to harvest livers, whose weights were immediately measured. Portions of liver tissue were fixed in 4% paraformaldehyde, and the remaining tissue was stored in cryovials in liquid nitrogen for subsequent use.

Hematoxylin-eosin (HE) staining of mouse liver tissues

Liver sections were stained with hematoxylin for 10 min, then rinsed in a gradient of ethanol solutions. Sections were then stained with 0.5% eosin for several min until the tissue turned red. Excess dye was removed by immersion in 95% ethanol for 5 min. After dehydration and clearing, sections were mounted with neutral balsam and observed under an upright microscope.

Serological detection in mice

Mouse blood was collected via eyeball enucleation into blood collection tubes, centrifuged at 3700×g for 15 min, and

the serum was harvested. Serum samples were sent to our hospital's clinical laboratory for analysis using an automatic biochemical analyzer to measure indicators, including alanine aminotransferase (ALT), aspartate aminotransferase (AST), triglycerides (TG), total cholesterol (TCh), alkaline phosphatase (ALP), high-density lipoprotein (HDL), and low-density lipoprotein (LDL). If immediate detection was not possible, serum was stored at -80 ˚C.

TUNEL assay for cell apoptosis (colorimetric method)

A biotin-labeled solution was prepared according to the kit instructions. Fifty microliters of the solution were added to each section (ensuring uniform coverage of the tissue sample) and incubated in a 37 ˚C oven for 1 hr. After incubation, sections were washed once with PBS, and 0.2 ml of the stop solution for the labeling reaction was added. Fifty microliters of Streptavidin-HRP working solution was added to the sections, followed by incubation at room temperature for 30 min. After PBS washing, 200 µl of DAB chromogen solution was added, and sections were incubated at room temperature for 5-30 min. After dehydration and clearing, sections were mounted with neutral balsam, and staining was observed.

Bioinformatics analysis of RNA-seq data

Transcriptome sequencing of AGXT2L1 KO and WT mice was performed by Shanghai Qiming Information Technology Co., Ltd. To identify differences between the two groups, differentially expressed genes (DEGs) were analyzed using Ballgown to determine significance (*P*-value), false discovery rate (Q-value), and fold change. DEGs were identified by comparing the experimental and control groups using the criteria $P<0.05$ and fold change>1.2.

Functional analysis of DEGs: Gene Ontology (GO) analysis was used to annotate the functions of DEGs using the GO database, identifying all biological processes associated with these genes. Fisher's exact test and multiple comparison tests were used to calculate the significance (*P*-value) and false discovery rate (FDR) for each function. Significant functions were identified using the criterion P-value<0.05.

Pathway analysis of DEGs: Pathway analysis was performed based on the Kyoto Encyclopedia of Genes and Genomes (KEGG) database. Fisher's exact test and chi-square test were used to analyze the significance of pathways involving target genes. Significant pathways were identified using the criterion $P<0.05$.

Statistical analysis

Experimental results were analyzed using SPSS 24.0 software. Quantitative data were expressed as mean±standard deviation ($\bar{x}\pm s$), and categorical data were expressed as counts and percentages. Quantitative data were compared using t-tests, and categorical data were analyzed using chi-square tests. A P-value<0.05 was considered statistically significant. All experiments were repeated at least three times.

Results

AGXT2L1 expression is decreased in multiple liver diseases

Public expression profiles of AGXT2L1 in liver diseases were downloaded from the NCBI database: alcoholic hepatitis (GDS4389, 7 normal liver tissue samples, 15 alcoholic hepatitis samples)(Figure 1A), HBV-related acute liver failure (GDS4387, 10 normal samples, 17 HBV-related acute liver failure samples)(Figure 1B), and high-fat diet-induced liver injury in mice (GDS4783, 18 normal diet samples, 18 high-fat diet samples)(Figure 1C). Statistical analysis of AGXT2L1 expression in these datasets showed that AGXT2L1 was abnormally downregulated in alcoholic hepatitis, HBV-related acute liver failure, and high-fat diet-induced liver injury compared with normal liver tissue ($P<0.05$)(Figure 1D).

Based on public expression profiles, clinical tissue

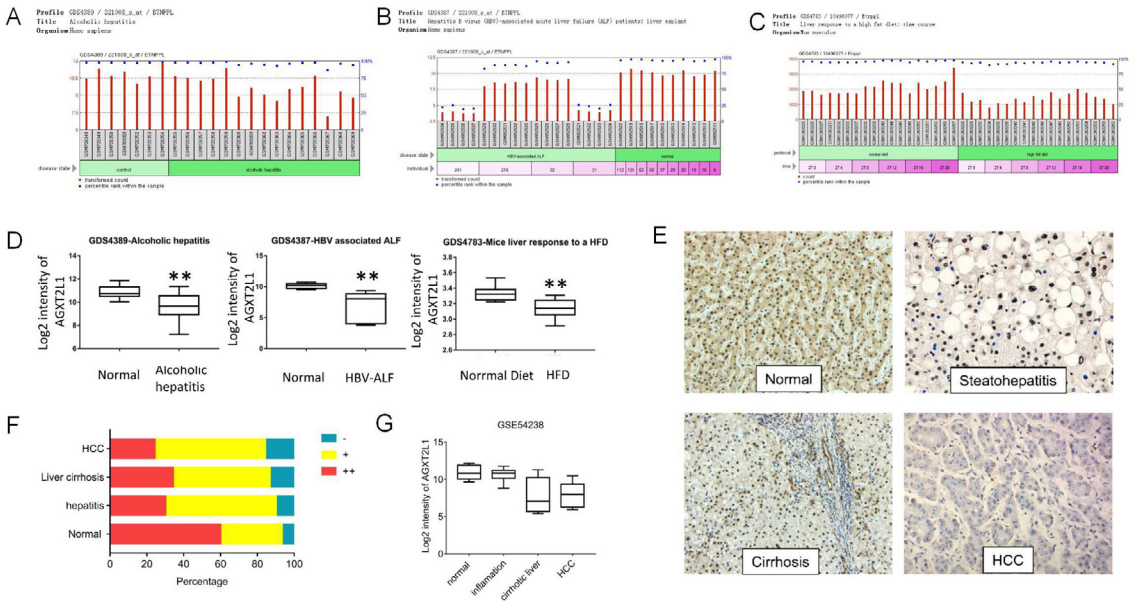

Figure 1. AGXT2L1 shows abnormally low expression in various liver diseases in mice
(A-C) Data from the NCBI public expression profile, respectively representing alcoholic hepatitis, HBV-related acute liver failure, and a mouse fatty liver model induced by a high-fat diet. (D)Statistical analysis of AGXT2L1 expression in three liver diseases from the database. (E) Immunohistochemical results of human normal liver tissue, steatotic liver tissue, cirrhotic liver tissue, and hepatocellular carcinoma tissue. (F) Statistical chart generated based on the scoring of immunohistochemical results. (G) mRNA expression of AGXT2L1 in normal liver tissue, chronic hepatitis tissue, cirrhotic liver tissue, and liver cancer tissue from the GSE54238 dataset
AGXT2L1: Alanine-glyoxylate aminotransferase; HBV: Hepatitis B virus

samples (including normal liver, cirrhotic, and steatotic liver tissues) were collected to investigate AGXT2L1 expression. Immunohistochemical analysis revealed AGXT2L1 protein expression in both the cytoplasm and nucleus, consistent with previous reports. As shown in Figure 1E, immunohistochemical scoring demonstrated that: (1) In hepatocellular carcinoma tissue microarrays (80 samples), AGXT2L1 expression was significantly lower in 70 hepatocellular carcinoma samples than in 10 normal liver tissue samples (P<0.01); (2) In cirrhosis tissue microarrays (70 samples), AGXT2L1 expression was significantly lower in 40 cirrhotic tissue samples than in 30 normal liver tissue samples (P<0.01); (3) In 20 steatotic liver tissue samples and matched normal liver tissue samples, AGXT2L1 expression was significantly lower in steatotic tissue. Immunohistochemical scoring (Figure 1F) and statistical analysis of the GSE54238 dataset (Figure 1G) further showed a gradual decrease in AGXT2L1 mRNA expression from normal liver tissue to chronic hepatitis, cirrhosis, and hepatocellular carcinoma. These results suggest that decreased AGXT2L1 expression may be characteristic of MCD diet-induced NAFLD and associated with disease progression.

AGXT2L1 expression is downregulated after induction of cellular steatosis in vitro and in vivo

An oleic acid-induced hepatocellular steatosis model was established using the HepG2 cell line. Based on the literature, HepG2 cells were treated with three concentrations of oleic acid: 0, 0.3, and 0.6 μg/ml. After 24 hr, Oil Red O staining revealed extensive lipid droplet formation in HepG2 cells treated with 0.6 μg/ml oleic acid (Figures 2A, 2B). Western Blot analysis showed that AGXT2L1 expression was significantly decreased in HepG2 cells treated with 0.6 μg/mL oleic acid (P<0.05)(Figures 2C, 2D). *In vitro* cell experiments further confirmed that steatosis inhibits AGXT2L1 expression in hepatocytes.

To verify that AGXT2L1 is a key regulator throughout NAFLD progression, animal experiments were conducted using 8-week-old male WT C57BL/6 mice. The experimental group was fed a high-fat diet, and the control group was fed a normal diet. Mice were sacrificed after 4 weeks of modeling. HE and Oil Red O staining of mouse liver tissues (Figure 2E) showed significant steatohepatitis in the MCD diet group, with more intense Oil Red O staining (indicating more lipid droplets) than in the control group. Immunohistochemical and western blot analysis of liver tissues from experimental and control mice showed significantly decreased AGXT2L1 protein expression in mice with steatohepatitis (Figure 2F). Quantitative real-time PCR (qRT-PCR) also revealed a significant decrease in AGXT2L1 mRNA expression in steatotic mice (P<0.01)(Figure 2G).

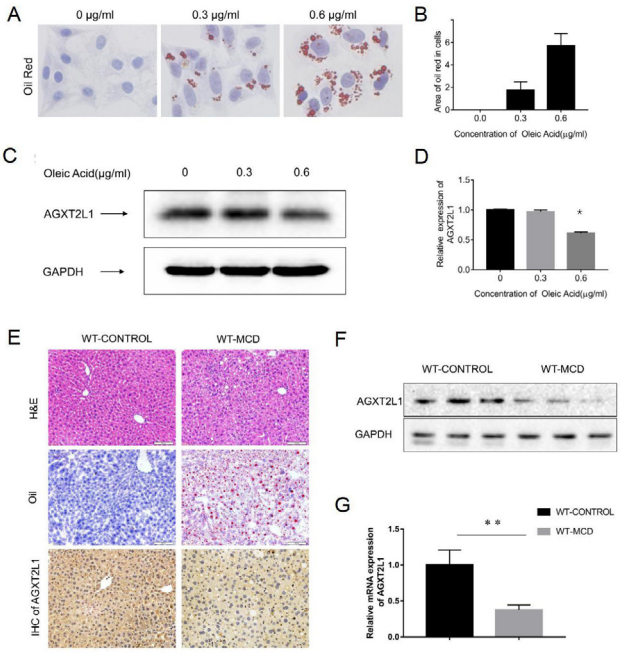

Figure 2. AGXT2L1 expression is down-regulated after inducing cellular steatosis in mouse *in vitro* and *in vivo* experiments
(A, B) Oleic acid at different concentrations (0, 0.3, 0.6 μg/ml) induces varying degrees of steatosis in HepG2 cells. (C, D) Western blot analysis shows that the expression level of AGXT2L1 in steatotic HepG2 cells is significantly decreased. (E) Sequentially showing the HE staining, Oil Red staining, and AGXT2L1 immunohistochemical results of liver tissues from mice fed a normal diet and an MCD diet. (F, G) Western Blot and QPCR results of AGXT2L1 in liver tissues from mice fed a normal diet and an MCD diet; *Indicates P<0.05
AGXT2L1: Alanine-glyoxylate aminotransferase; HE: Hematoxylin-Eosin staining; MCD: Methionine-choline-deficient

AGXT2L1 Knockout Mice Develop Spontaneous Liver Injury Starting at Three Months of Age

AGXT2L1 knockout mice (Agxt2l1$^{-/-}$; KO) were generated using CRISPR/Cas9 gene-editing technology; wild-type mice (WT) served as controls. To observe whether KO mice develop pathological changes due to reduced AGXT2L1 expression, three KO and three WT mice were randomly selected monthly, sacrificed after blood collection, and their livers were harvested. Serum levels of ALT, AST, ALP, TG, and TCh were measured, and liver tissues were subjected to HE staining to assess pathological changes. As shown in Figure 3A, HE staining of KO mouse livers revealed

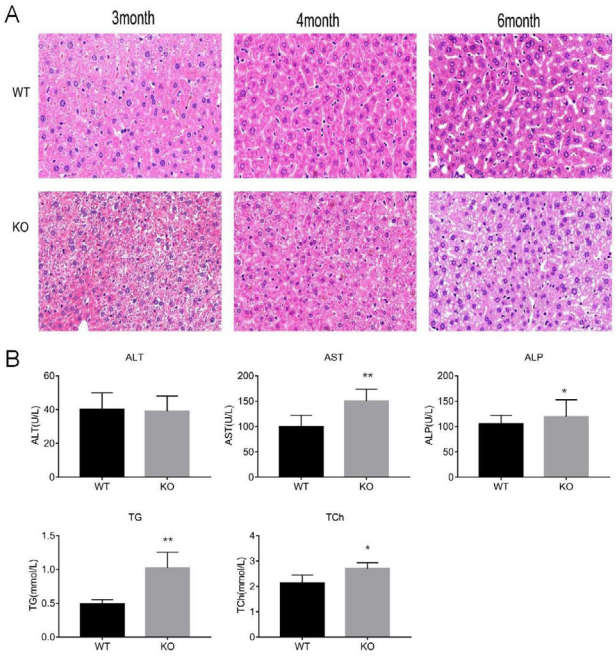

Figure 3. Hepatic steatosis occurs in the livers of KO mice
(A)Upper panel shows the HE staining results of liver tissues from 3-, 4-, and 6-month-old WT mice; Lower panel shows the HE staining results of liver tissues from 3-, 4-, and 6-month-old KO mice. (B) Levels of serum ALT, AST, ALP, TG, and TCh in 3-month-old KO and WT mice
WT: Wild-type; KO: AGXT2L1 knockout. ALT: Alanine Aminotransferase; AST: Aspartate Aminotransferase; ALP: Alkaline Phosphatase; TG: Triglycerides; TCh: Total Cholesterol

steatosis starting at 3 months of age, which persisted at 4 and 6 months; WT mouse livers remained normal. At 3 months, serum levels of ALT, AST, ALP, TG, and TCh were abnormally elevated in KO mice compared with WT mice (Figure 3B). These findings suggest that reduced AGXT2L1 expression in mouse livers increases serum levels of enzymes (e.g., ALT, AST) and lipids (e.g., TG, TCh), and induces pathological changes such as hepatocellular steatosis.

KO mice exhibit more severe hepatic steatosis than WT mice under MCD diet conditions

We previously confirmed that AGXT2L1 expression is significantly downregulated in steatotic livers. Next, KO and WT mice were fed an MCD diet to compare NASH severity. HE and Oil Red O staining (Figure 4A) showed that MCD diet-induced hepatic steatosis was more extensive and severe in KO mice than in WT mice (Figure 4B). These results indicate that AGXT2L1 deficiency increases susceptibility to steatohepatitis.

Serum samples from each group were collected to measure NASH-related serological indicators (Figure 4C). Serum levels of ALT, AST, and ALP were significantly higher in WT and KO mice fed an MCD diet than in those fed a normal diet; notably, these indicators were more significantly elevated in KO mice than in WT mice under MCD diet conditions (P<0.05). Serological data thus confirmed that Agxt2l1$^{-/-}$ mice develop more severe steatohepatitis than WT mice.

qRT-PCR was used to measure the mRNA expression of inflammation-related factors (TNF-α, TGF-β, IL-6, IL-10) in the livers of KO and WT mice fed normal or MCD diets; immunohistochemistry was performed to detect TNF-α and TGF-β in liver tissues. Consistent with the ALT and AST results, mRNA levels of pro-inflammatory factors (TNF-α, TGF-β, IL-6) were significantly elevated (and IL-10 was significantly decreased) in the livers of MCD-induced KO and WT mice, with higher levels observed in KO mice (Figure 4D). Immunohistochemical analysis of mouse liver tissues showed increased TNF-α and TGF-β expression in MCD-induced mice, with significantly stronger expression in KO mice than in WT mice (P<0.01)(Figure 4E). These results suggest that AGXT2L1 deficiency promotes the development of NAFLD.

Abnormal AGXT2L1 expression primarily affects phospholipid metabolism

To further explore the biological function of AGXT2L1, RNA sequencing and bioinformatics analysis were performed on AGXT2L1 KO and WT mice (n=3 per group; KO mice as the experimental group, WT mice as the control group).

Compared with the control group, the experimental group had 138 differentially expressed genes (DEGs), including 76 up-regulated and 62 downregulated genes. A total of 361 differential transcripts were identified between the KO and WT groups, including 224 up-regulated and 137 downregulated. Cluster analysis of samples and genes was performed using gene signal values, generating cluster maps of DEGs and differential transcripts (Figures 5A, 5B). Functional annotation of up-regulated DEGs revealed enrichment in 30 biological processes, primarily involving redox reactions and metabolic processes (including phospholipid metabolism, sterol biosynthesis/metabolism, and fatty acid biosynthesis/metabolism)(Figure 5C). KEGG pathway analysis of DEGs (screened with P<0.05) identified 60 significant pathways, including 30 pathways associated with up-regulated genes.

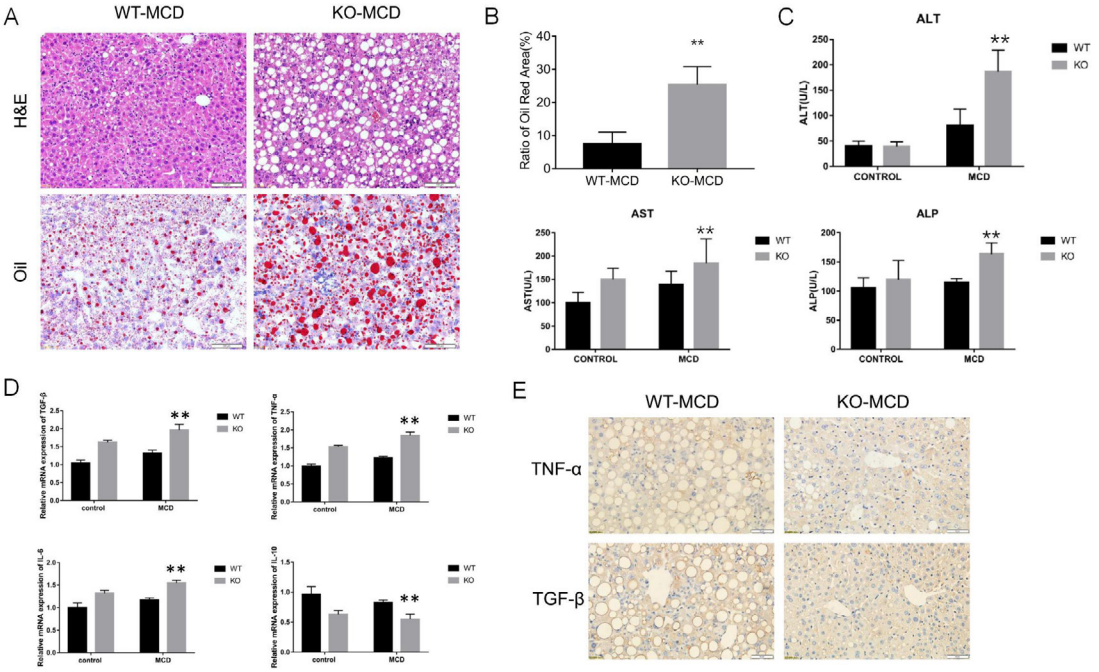

Figure 4. Mice under high-fat diet induction, Agxt2l1^{-}/$^{-}$ mice, develop more severe steatohepatitis than WT mice

(A) Hepatic pathological HE staining and Oil Red O staining of WT and KO mice after MCD diet induction. (B) Statistical analysis of the steatosis area from Oil Red O staining. (C) Serum indicators, including ALT, AST, and ALP, in KO and WT mice. (D) Quantitative real-time PCR (qPCR) detection of the mRNA expression levels of genes such as TNF-α, TGF-β, IL-6, and IL-10 in KO and WT mice under MCD diet and control diet conditions. (E) Immunohistochemical detection of the expression of TNF-α and TGF-β in liver tissues of WT and KO mice with steatohepatitis induced by MCD diet.*Indicates P<0.05

WT: wild-type; KO: AGXT2L1 knockout; ALT: Alanine Aminotransferase; AST: Aspartate Aminotransferase; ALP: Alkaline Phosphatase; TNF-α: Tumor Necrosis Factor-α; TGF-β: Transforming growth factor-β; IL-6: Interleukin-6; IL-10: Interleukin-10; WT: Wild-type; KO:AGXT2L1 knockout

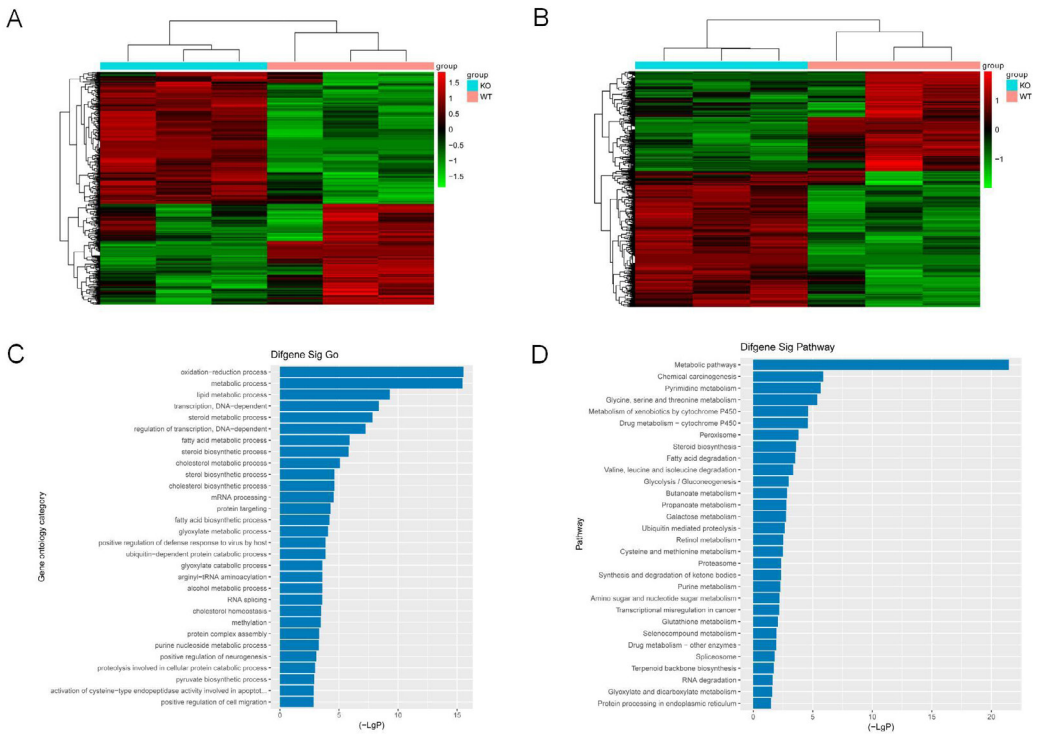

Figure 5. RNA sequencing analysis of AGXT2L1 knockout (KO) mice
(A) Cluster heatmap of differentially expressed genes (DEGs). (B)Cluster heatmap of differentially expressed transcripts. In the figure, red indicates that the differentially expressed genes are highly expressed in the inter-group samples. In contrast, green indicates low expression in the grouped samples. (C) Bar chart of functions of significantly up-regulated differentially expressed genes between the two groups of samples. (D) Pathway distribution map of significantly up-regulated differentially expressed genes between the two sample groups

The most prominent pathways were metabolism-related, with additional involvement of cytochrome P450 and lipid synthesis/metabolism pathways (Figure 5D). These results indicate that abnormal AGXT2L1 expression is primarily associated with phospholipid metabolism.

AGXT2L1 Deficiency promotes hepatocyte apoptosis and endoplasmic reticulum stress

To further explore the role of AGXT2L1 in NAFLD, TUNEL assays were performed to assess hepatocyte apoptosis in MCD-induced mice. As shown in Figures 6A and 6B, MCD-induced KO mice developed more severe steatohepatitis and had a higher number of apoptotic cells than WT mice.

qRT-PCR was used to measure the expression of endoplasmic reticulum stress marker genes (CHOP and PERK) in the livers of WT and KO mice. As shown in Figure 6C, MCD-induced steatohepatitis increased the expression of endoplasmic reticulum stress marker genes; notably, CHOP and PERK expression were more significantly elevated in KO mice than in WT mice ($P<0.05$).

These findings suggest that reduced AGXT2L1 expression promotes hepatocyte apoptosis and endoplasmic reticulum stress, thereby facilitating or exacerbating NAFLD progression.

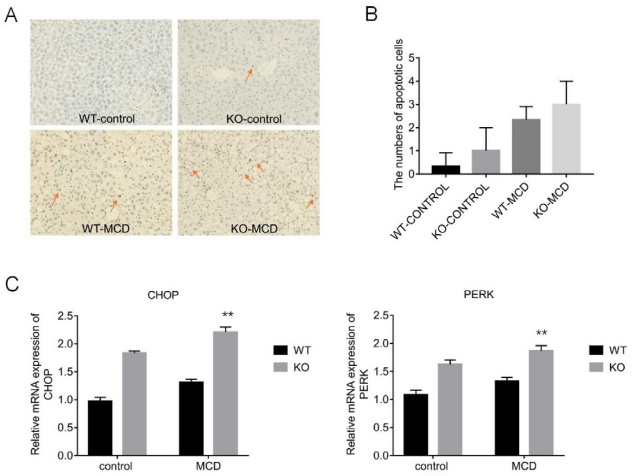

Figure 6. AGXT2L1 deficiency promotes hepatocyte apoptosis and endoplasmic reticulum stress
(A)The cells indicated by arrows in the figure are TUNEL-positive apoptotic cells. (B)Statistical count of hepatocyte apoptosis in mice after steatohepatitis induction by MCD diet. (C) Real-Time PCR detection of the expression of endoplasmic reticulum stress marker genes CHOP and PERK in the livers of WT and KO mice. Control group: Fed with a normal diet; MCD group: Fed with an MCD diet
WT: Wild-type; KO: AGXT2L1 knockout. CHOP: C/EBP homologous protein; PERK: Protein kinase R-like endoplasmic reticulum kinase

Discussion

Previous studies on AGXT2L1 have focused on its association with brain tissue and psychiatric disorders (23, 24). This study is the first to extend AGXT2L1 research to liver diseases, identifying decreased AGXT2L1 expression as a "common phenomenon" in liver injury. This cross-system finding overcomes the limitations of traditional gene function research and offers a new perspective on tissue-specific gene function.

More importantly, using an AGXT2L1-/- mouse model, this study indicated a possible association between reduced AGXT2L1 expression and spontaneous hepatic steatosis *in vivo*—consistent with *in vitro* findings that "down-regulated AGXT2L1 expression promotes lipid accumulation." The study clarifies that reduced AGXT2L1 expression promotes

NAFLD through three interconnected pathways linked by PE metabolism, forming a complete "gene-metabolism-pathology" chain:

Activation of inflammatory responses: Reduced AGXT2L1 expression may increase PE levels and decrease the PC/PE ratio, enhancing hepatocyte membrane permeability and releasing intracellular contents. This activates Kupffer cells, recruits neutrophils and macrophages, and triggers an inflammatory cascade that exacerbates hepatocyte injury—a core feature of NAFLD progression to NASH.

Promotion of hepatocyte apoptosis: Disrupted membrane integrity (caused by PC/PE imbalance) may directly trigger apoptotic signaling. Additionally, pro-inflammatory cytokines (e.g., TNF-α, IL-6) released during inflammation may further induce apoptosis, forming a "damage-apoptosis" vicious cycle.

Enhancement of endoplasmic reticulum stress: PC and PE are key regulators of the "unfolded protein response" during endoplasmic reticulum stress. An imbalanced PC/PE ratio may induce endoplasmic reticulum stress, which not only exacerbates apoptosis but also disrupts lipid metabolism (e.g., promoting triglyceride synthesis), accelerating NAFLD progression.

This study has two key implications: First, our findings suggest that AGXT2L1 may be tentatively linked to NAFLD, which might help expand the potential molecular regulatory network of NAFLD (previous studies have primarily focused on classic lipid metabolism-related genes such as PPARγ and SREBP-1c)(25, 26). Second, AGXT2L1 may serve as a potential biomarker for NAFLD (its expression level reflects the degree of liver injury) or a therapeutic target (up-regulating AGXT2L1 may improve PE metabolism imbalance). Additionally, PE metabolism-related pathways (e.g., PE synthases, PC/PE ratio-regulating enzymes) may represent new directions for drug development, providing a theoretical basis for targeted NAFLD therapy.

This study also has limitations, such as the lack of PE detection. A reduced PC/PE ratio is both a "cause" of membrane damage and a "consequence" of endoplasmic reticulum stress, and is a key metabolic node linking inflammation and apoptosis. Another limitation of the present study is the differences and limitations between the MCD diet-induced animal model and human NAFLD. Although the MCD diet model is widely used to induce NASH-like pathological changes in animal experiments because it rapidly induces hepatic steatosis, inflammation, and fibrosis, it differs from human NAFLD/NASH in several key aspects that were not fully addressed in this study.

Future studies will explore the mechanism by which AGXT2L1 regulates PE metabolism imbalance, providing a new molecular explanation for "how lipidome imbalance drives liver disease progression."

Conclusion

This study is the first to extend research on AGXT2L1 from brain tissue and psychiatric disorders to liver diseases, identifying decreased AGXT2L1 expression as a clear alteration in liver injury. Using a gene knockout mouse model and other approaches, the study confirms that reduced AGXT2L1 expression promotes NAFLD through three pathways: activation of inflammatory responses, promotion of hepatocyte apoptosis, and enhancement of endoplasmic reticulum stress. This finding expands the molecular regulatory network of NAFLD, suggesting that AGXT2L1 may serve as a biomarker, therapeutic target, and guide for drug development.

Acknowledgment

This work was supported by the Medical Scientific Research Foundation of Guangdong Province, China (Grant No. A2024736) and the Science and Technology Projects of Guangzhou, China (Grant No. 2024A04J5236).

Authors' Contributions

L W designed the experiments; supervised, directed, and managed the study; Y Y performed experiments, collected data, conducted analysis and interpretation of results, and drafted the manuscript; Y Y and L W approved the final version for publication.

Conflicts of Interest

The authors have no competing interests to declare that are relevant to the content of this article.

Declaration

We have not used any AI tools or technologies to prepare this manuscript.

References

1. Quek J, Chan KE, Wong ZY, Tan C, Tan B, Lim WH, *et al.* Global prevalence of non-alcoholic fatty liver disease and non-alcoholic steatohepatitis in the overweight and obese population: A systematic review and meta-analysis. Lancet Gastroenterol Hepatol 2023; 8: 20-30.
2. Devarbhavi H, Asrani SK, Arab JP, Nartey YA, Pose E, Kamath PS. Global burden of liver disease: 2023 update. J Hepatol 2023; 79: 516-537.
3. Powell EE, Wong VW, Rinella M. Non-alcoholic fatty liver disease. Lancet 2021; 397: 2212-2224.
4. Teng ML, Ng CH, Huang DQ, Chan KE, Tan DJ, Lim WH, *et al.* Global incidence and prevalence of nonalcoholic fatty liver disease. Clin Mol Hepatol 2023; 29: S32-S42.
5. Friedman SL, Neuschwander-Tetri BA, Rinella M, Sanyal AJ. Mechanisms of NAFLD development and therapeutic strategies. Nat Med 2018; 24: 908-922.
6. Grander C, Grabherr F, Tilg H. Non-alcoholic fatty liver disease: Pathophysiological concepts and treatment. Cardiovasc Res 2023; 119: 1787-1798.
7. Tilg H, Moschen AR. Evolution of inflammation in nonalcoholic fatty liver disease: The multiple parallel hits hypothesis. Hepatology 2010; 52: 1836-1846.
8. Tilg H, Adolph TE, Moschen AR. Multiple parallel hits hypothesis in nonalcoholic fatty liver disease: Revisited after a decade. Hepatology 2021; 73: 833-842.
9. Van der Veen JN, Kennelly JP, Wan S, Vance JE, Jacobs RL, Vance DE. The critical role of phosphatidylcholine and phosphatidylethanolamine metabolism in health and disease. Biochim Biophys Acta Biomembr 2017; 1859: 1558-1572.
10. Rong S, Xia M, Vale G, Wang S, Kim CW, Li S, *et al.* DGAT2 inhibition blocks SREBP-1 cleavage and improves hepatic steatosis by increasing phosphatidylethanolamine in the ER. Cell Metab 2024; 36: 617-629.
11. Petkevicius K, Palmgren H, Glover MS, Ahnmark A, Andréasson AC, Madeyski-Bengtson K, *et al.* TLCD1 and TLCD2 regulate cellular phosphatidylethanolamine composition and promote the progression of non-alcoholic steatohepatitis. Nat Commun 2022; 13: 6020.
12. Gibellini F, Smith TK. The Kennedy pathway--*De novo* synthesis of phosphatidylethanolamine and phosphatidylcholine. IUBMB Life 2010; 62: 414-428.

13. Ballesteros U, González-Ramirez EJ, de la Arada I, Sot J, Etxaniz A, Goñi FM, *et al.* Effects of a N-maleimide-derivatized phosphatidylethanolamine on the architecture and properties of lipid bilayers. Int J Mol Sci 2023; 24: 16570.
14. Korbecki J, Bosiacki M, Kupnicka P, Barczak K, Ziętek P, Chlubek D, *et al.* Biochemistry and diseases related to the interconversion of phosphatidylcholine, phosphatidylethanolamine, and phosphatidylserine. Int J Mol Sci 2024; 25: 10745.
15. Vance JE. Phospholipid synthesis and transport in mammalian cells. Traffic 2015; 16: 1-18.
16. Shama S, Jang H, Wang X, Zhang Y, Shahin NN, Motawi TK, *et al.* Phosphatidylethanolamines are associated with nonalcoholic fatty liver disease (NAFLD) in obese adults and induce liver cell metabolic perturbations and hepatic stellate cell activation. Int J Mol Sci 2023; 24: 1034.
17. Veiga-da-Cunha M, Hadi F, Balligand T, Stroobant V, Van Schaftingen E. Molecular identification of hydroxylysine kinase and of ammoniophospholyases acting on 5-phosphohydroxy-L-lysine and phosphoethanolamine. J Biol Chem 2012; 287: 7246-7255.
18. Schiroli D, Cirrincione S, Donini S, Peracchi A. Strict reaction and substrate specificity of AGXT2L1, the human O-phosphoethanolamine phospho-lyase. IUBMB Life 2013; 65: 645-650.
19. Ding Q, Kang J, Dai J, Tang M, Wang Q, Zhang H, *et al.* AGXT2L1 is down-regulated in hepatocellular carcinoma and associated with abnormal lipogenesis. J Clin Pathol 2016; 69: 215-220.
20. Hernández-Alvarez MI, Sebastián D, Vives S, Ivanova S, Bartoccioni P, Kakimoto P, *et al.* Deficient endoplasmic reticulum-mitochondrial phosphatidylserine transfer causes liver disease. Cell 2019; 177: 881-895.
21. Deng Y, Wu L, Ding Q, Yu H. AGXT2L1 is downregulated in carcinomas of the digestive system. Oncol Lett 2020; 20: 1318-1326.
22. Aissa AF, Tryndyak V, de Conti A, Melnyk S, Gomes TD, Bianchi ML, *et al.* Effect of methionine-deficient and methionine-supplemented diets on the hepatic one-carbon and lipid metabolism in mice. Mol Nutr Food Res 2014; 58: 1502-1512.
23. Shao L, Vawter MP. Shared gene expression alterations in schizophrenia and bipolar disorder. Biol Psychiatry 2008; 64: 89-97.
24. Schillaci FA, Lanza G, Salluzzo MG, L'Episcopo F, Ferri R, Salemi M. The role of ETNPPL in dopaminergic neuron stability: Insights from neuromelanin-associated protein expression in Parkinson's disease. Int J Mol Sci 2024; 25: 13107.
25. Pawlak M, Lefebvre P, Staels B. Molecular mechanism of PPAR action and its impact on lipid metabolism, inflammation and fibrosis in non-alcoholic fatty liver disease. J Hepatol 2015; 62: 720-733.
26. Chen H, Tan H, Wan J, Zeng Y, Wang J, Wang H, *et al.* PPAR-γ signaling in nonalcoholic fatty liver disease: Pathogenesis and therapeutic targets. Pharmacol Ther 2023; 245: 108391.